Electronic Supplementary Material (ESI) for Chemical Communications

Substituent and counterion effects on the formation of π-bound dimers from one-electron oxidized end-capped heptathienoacenes‡

Cristina Capel Ferrón,[a] M. Carmen Ruiz Delgado,*[a] Víctor Hernández,*[a] Juan T. López Navarrete,*[a] Barbara Vercelli,[b] Gianni Zotti,[b] Marçal Capdevila Cortada,[c] Juan J. Novoa,*[c] Weijun Niu,[d] Mingqian He,[d] František Hartl*[e]

Figure S1.- Cyclic voltammograms of $2x10^{-4}$ M **TIPS-T7-TIPS** and **D4T7** recorded at 293 K in CH_2Cl_2 containing 0.1 M Bu_4NClO_4, at the scan rate of 100 mV/s. The working electrode was a Pt microdisc and the reference electrode an Ag/0.1 M Ag^+ (+0.34 V vs SCE).

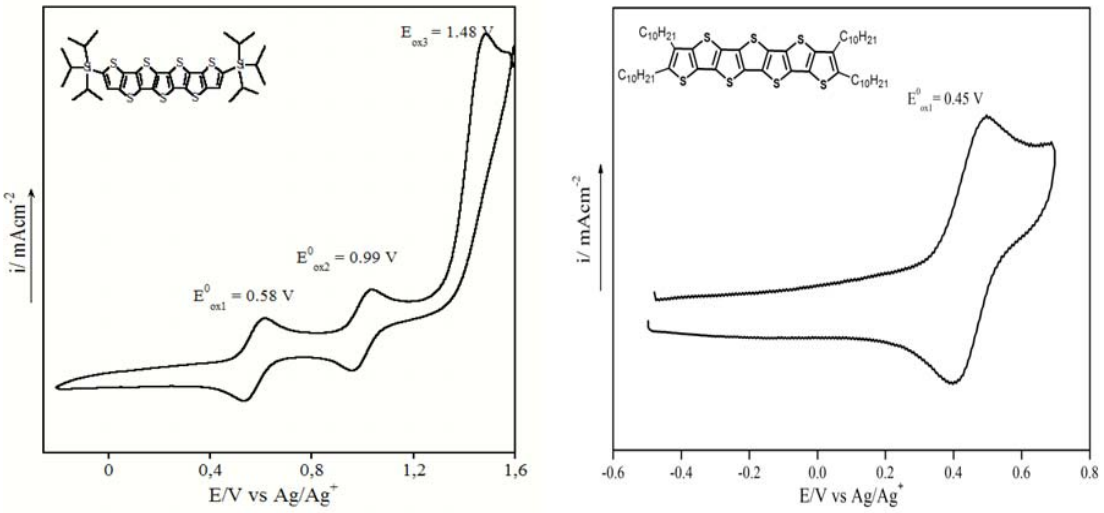

Figure S2.- DFT//M06L/6-31G(d) energy levels around the HOMO-LUMO band gap region and molecular orbital topologies of the HOMO and LUMO of **D4T7** (left) and **TIPS-T7-TIPS** (right).

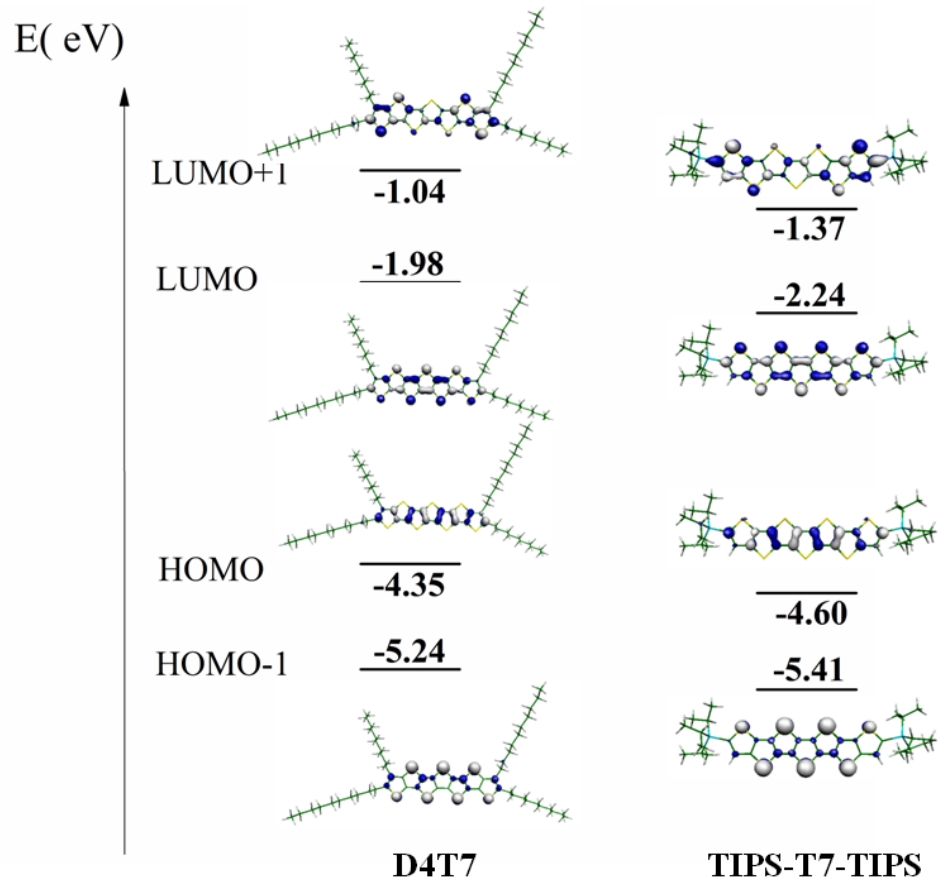

Figure S3.- Lateral and top views of the optimum geometry of the antiparallel u-u-u-u **[D4T7$^{\bullet+}$]$_2$**$(CH_2Cl_2)_8$ aggregate computed at the M06L/6-31G(d) level.

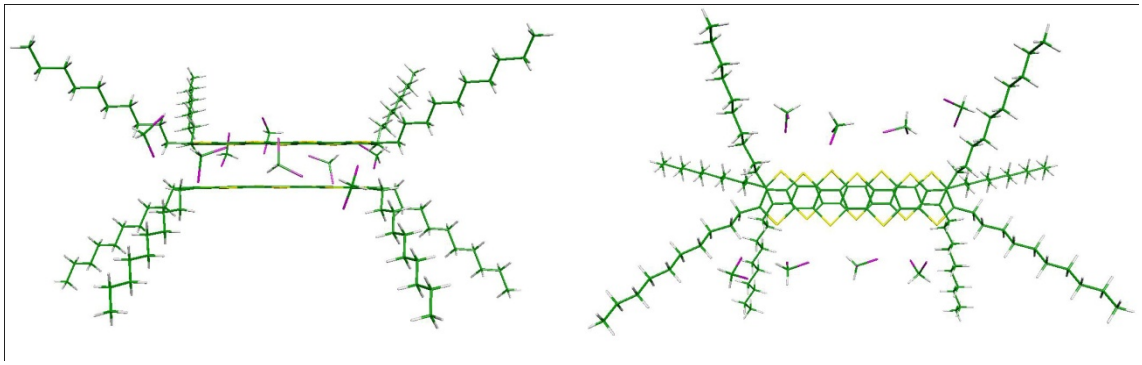

Figure S4.- Lateral and top views of the optimum geometry of the parallel u-u-u-u **[D4T7$^{\bullet+}$]$_2$**(CH_2Cl_2)$_8$ aggregate computed at the M06L/6-31G(d) level.

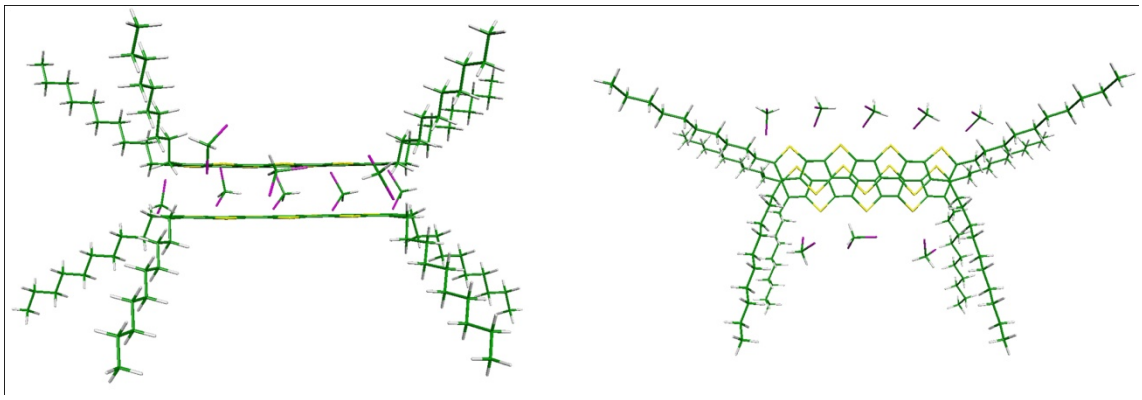

Figure S5.- Lateral and top views of the optimum geometry of the antiparallel u-d-u-d **[D4T7$^{\bullet+}$]$_2$**$(CH_2Cl_2)_8$ aggregate computed at the M06L/6-31G(d) level.

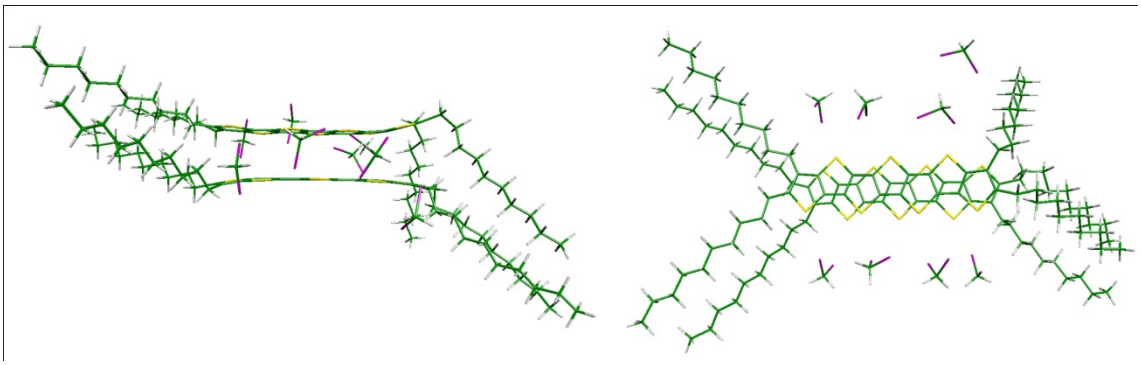

Figure S6.- Lateral and top views of the optimum geometry of the parallel u-d-u-d **[D4T7$^{\bullet+}$]$_2$**$(CH_2Cl_2)_8$ aggregate computed at the M06L/6-31G(d) level.

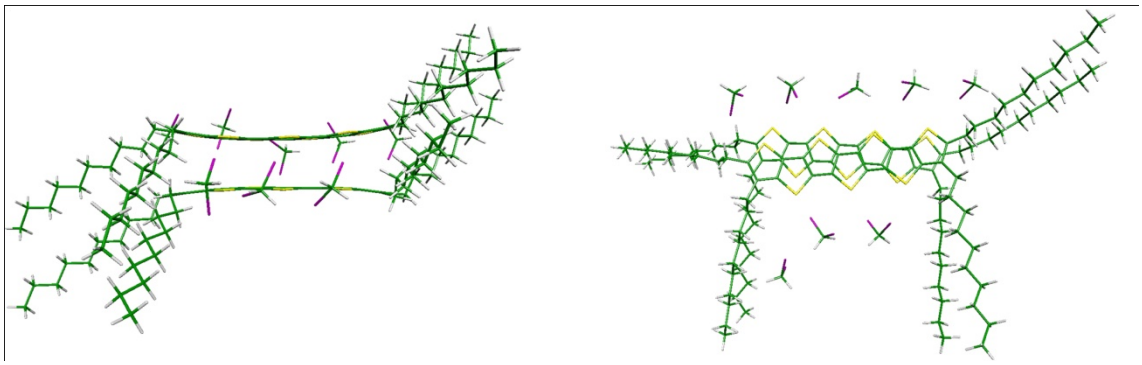

Figure S7.- Lateral and top views of the optimum geometry of the antiparallel u-u-u-u **[D4T7$^{\bullet+}$]$_2$**(PF_6^-)$_2$ aggregate computed at the M06L/6-31G(d) level. The shortest inter-radical C•••C distance, 3.24 Å, is also indicated.

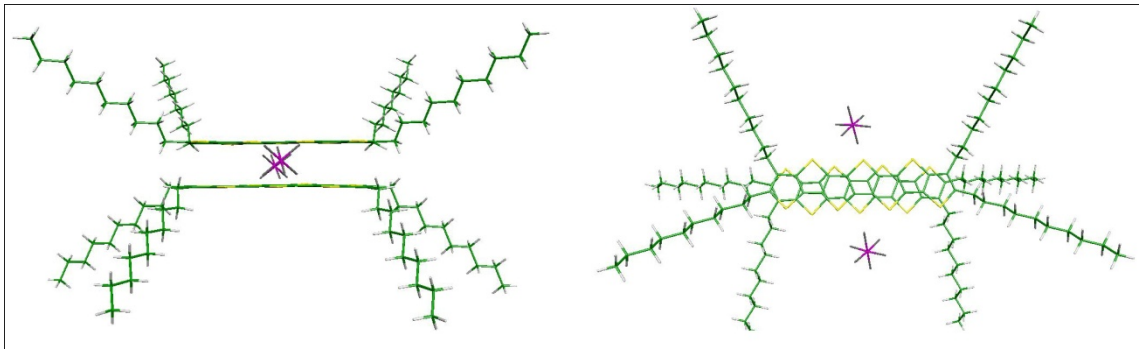

Figure S8.- Lateral and top views of the optimum geometry of the parallel u-u-u-u **[D4T7$^{\bullet+}$]$_2$**(PF_6^-)$_2$ aggregate computed at the M06L/6-31G(d) level.

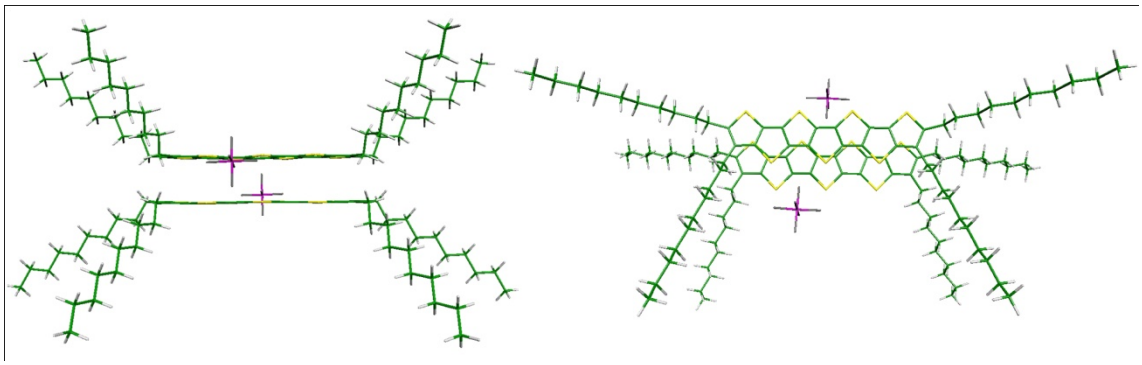

Figure S9.- HOMO (right) and LUMO orbitals (left) for the optimum geometry of the antiparallel u-u-u-u **[D4T7$^{\bullet+}$]$_2$**$(CH_2Cl_2)_8$ aggregate computed at the M06L/6-31G(d) level.

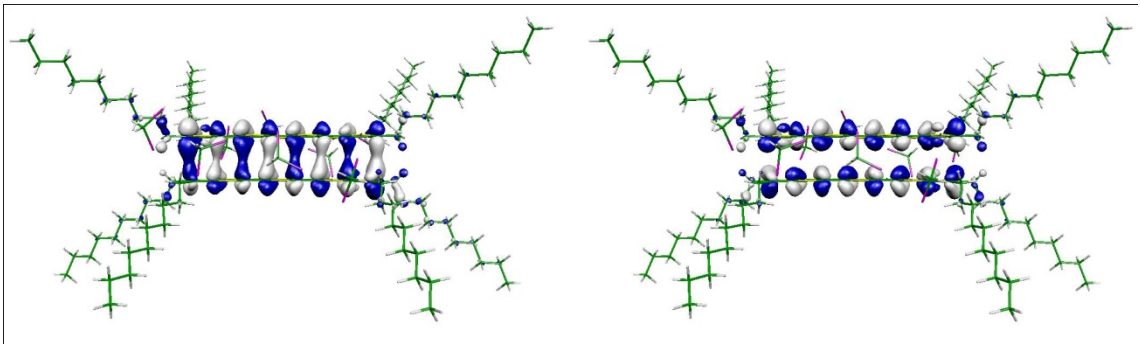

Figure S10.- HOMO (right) and LUMO orbitals (left) for the optimum geometry of the antiparallel u-u-u-u **[D4T7$^{\bullet+}$]$_2$**(PF_6^-)$_2$ aggregate computed at the M06L/6-31G(d) level.

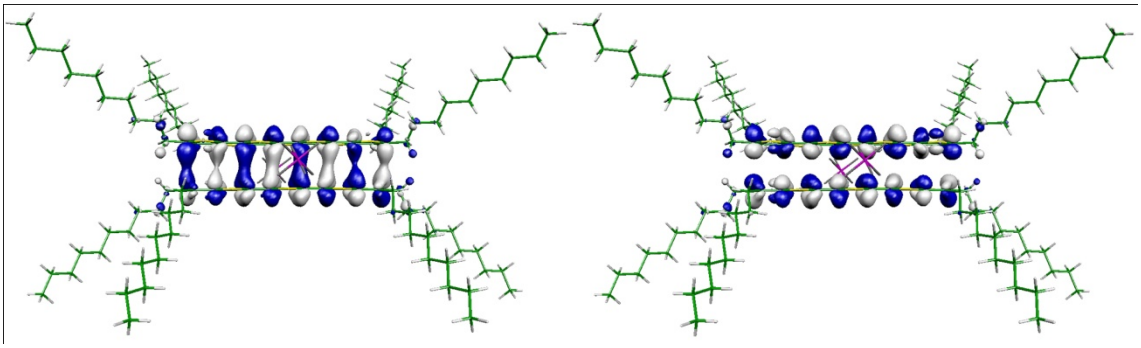

Table S1.- TDDFT//M06L/6-31G(d) vertical one-electron excitations [nm] representing the strong Vis-NIR absorptions of **D4T7**$^{\bullet+}$, with oscillator strengths in parentheses. HOMO, SOMO (singly occupied molecular orbital) and LUMO are abbreviated as H, S and L, respectively. The α,β notation refers to the unpaired (α spin).and paired (β spin) electrons.

	Experiment	TDDFT	Description
D4T7$^{\bullet+}$	582	524 (1.3)	$S_\alpha \rightarrow L_\alpha$
	1116	967 (0.4)	$(H_\beta \rightarrow L_\beta)+(H_{\beta-1} \rightarrow L_\beta)+(S_\alpha \rightarrow L_\alpha)$

Table S2.- Lowest energy electronic transitions, computed at the TDDFT//M06L/6-31G(d) levels, for the antiparallel (AP) and parallel (P) **[D4T7$^{\bullet+}$]$_2$**$(CH_2Cl_2)_8$ and **[D4T7$^{\bullet+}$]$_2$**$(PF_6^-)_2$ aggregates, at their optimum M06L/6-31G(d) geometries. The oscillator strength value for each electronic transition is provided within parenthesis.[a]

Conformation	TDDFT//M06L Electronic transitions (nm)			
AP [**D4T7**$^{\bullet+}$]$_2$$(CH_2Cl_2)_8$	976 (0.2) H → L	917 (0.3) (H-5 → L) + (H-2 → L) + (H-3 → L) + (H-1 → L)	813 (0.2) (H-12 → L) + (H-11 → L) + (H-1 → L) + (H-5 → L)	
AP [**D4T7**$^{\bullet+}$]$_2$$(PF_6^-)_2$	929 (0.2) H → L	770 (0.8) H-2 → L	435 (0.2) H → L+2	433 (1.4) (H → L+1) + (H-20 → L)
P [**D4T7**$^{\bullet+}$]$_2$$(CH_2Cl_2)_8$	1241 (0.2) H → L	1035 (0.2) (H-2 → L) + (H-3 → L) + (H-4 → L)	830 (0.2) H-18 → L	823 (0.2) (H-18 → L) + (H-1 → L) + (H-12 → L)
P [**D4T7**$^{\bullet+}$]$_2$$(PF_6^-)_2$	1176 (0.2) H → L	789 (0.7) (H-3 → L) + (H-2 → L)	461 (0.4) H-18 → L	454 (0.3) (H → L+2) + (H-19 → L)

[a]HOMO, SOMO (singly occupied molecular orbital) and LUMO are abbreviated as H, S and L, respectively.

Table S3.- Lowest energy electronic transitions, computed at the CIS/6-31G(d) level, for the antiparallel (AP) and parallel (P) **[D4T7$^{\bullet+}$]$_2$**$(CH_2Cl_2)_8$ and **[D4T7$^{\bullet+}$]$_2$**$(PF_6^-)_2$ aggregates, at their optimum M06L/6-31G(d) geometries together with those for the isolated radical cation. The oscillator strength value for each electronic transition is provided within parenthesis.[a]

Conformation	CIS Electronic transitions (nm)		
AP [**D4T7**$^{\bullet+}$]$_2(CH_2Cl_2)_8$	870 (0.4) H → L	578 (1.9) H-1 → L	341 (3.7) H → L+1
AP [**D4T7**$^{\bullet+}$]$_2(PF_6^-)_2$	853 (0.4) H → L	535 (0.8) 514 (1.0) (H-1 → L) + (H-2 → L)	335 (3.7) H → L+1
P [**D4T7**$^{\bullet+}$]$_2(CH_2Cl_2)_8$	1173 (0.3) H → L	591 (1.8) H-1 → L	357 (3.6) H → L+1
P [**D4T7**$^{\bullet+}$]$_2(PF_6^-)_2$	1146 (0.4) H → L	550 (0.7) 540 (0.6) (H-1 → L) + (H-2 →L)	349 (3.9) H → L+1
[**D4T7**$^{\bullet+}$][b]	514 (1.3) Hβ → Lβ	403 (0.3) Sα → Lα	

[a]HOMO, SOMO (singly occupied molecular orbital) and LUMO are abbreviated as H, S and L, respectively. [b]The α notation is related to the unpaired (α spin) electron.

Experimental details

Chemicals and reagents

Dichloromethane was freshly distilled from CaH_2 under a dry nitrogen atmosphere. The supporting electrolytes Bu_4NPF_6 and Bu_4NClO_4 (Aldrich) were recrystallized twice from absolute ethanol and vacuum-dried at 80 °C overnight.

The heptathienoacene capped with triisopropylsilyl (TIPS) or *n*-decyl substituents in the α and/or β terminal positions have been prepared according to the literature.[1-3] Thianthrenium radical cation PF_6^- salt ($TAPF_6$) has been prepared following the method of Ref. 4.

Electrochemical apparatus and procedure

Cyclic voltammograms were performed at 298 K under nitrogen in a three-electrode cell. The working electrode was a platinum microdisc (0.003 cm^2). The counter electrode was a platinum sheet. The reference electrode was a silver/0.1 M silver perchlorate in acetonitrile (0.34 V vs SCE). The voltammetric apparatus (AMEL, Italy) consisted of a Model 551 potentiostat modulated by a Model 568 programmable function generator and coupled to a Model 731 digital integrator.

UV-Vis-NIR spectroelectrochemistry was carried at 293 K, using an optically transparent thin-layer electrochemical cell[5] positioned in the sample compartment of a Scinco S3100 diode array spectrophotometer. The working electrode (Pt minigrid, 32 wires per cm) potential was controlled with a PA4 potentiostat (Laboratory devices, Polná, Czech Republic).

Conventional UV-Vis-NIR spectra were recorded in a 10-mm quartz cell (Hellma) on a Cary 5000 UV-Vis-NIR spectrophotometer at room temperature (ca. 298 K). Aliquots of a freshly prepared thianthrenium radical cation PF_6^- salt ($TAPF_6$) solution in CH_2Cl_2 were added stepwise to the sample solution in the cuvette. After each addition, a UV-Vis-NIR spectrum was recorded.

[1]M. He, F. Zhang, *J. Org. Chem.* 2007, ***72***, 442.

[2]T. Okamoto, K. Kudoh, A. Wakamiya, S. Yamaguchi, *Org. Lett.,* 2005, ***7***, 5301.

[3]X.Zhang, A.P. Côté, A. J. Matzger, *J. Am. Chem. Soc.* 2005, **127**, 10502

[4]Johannes Beck, Thomas Bredow, Rachmat Triandi Tjahjanto, *Z. Naturforsch.* 2009, **64b**, 145.

[5]M. Krejčík, M. Daněk, F. Hartl, *J. Electroanal. Chem. Interfacial Electrochem.* 1991, **317**, 179.

Computational details

Density Functional Theory (DFT) calculations were carried out by means of the Gaussian 09 program[1] running on SGI Origin 2000 supercomputer. The M06L functional[2] and the standard 6-31G(d) basis set were used.[3] Vertical electronic excitation energies were computed by using the time-dependent DFT (TDDFT) approach[4,5] and single-excitation configuration interaction (CIS) method.[6] TDDFT and CIS calculations were carried out using the M06L functional and the 6-31G(d) basis set on the previously optimized molecular geometries obtained at the same level of calculation. Molecular orbital contours were plotted using Molekel 4.3.[7]

[1] Gaussian 09, Revision B.01, M. J. Frisch, G. W. Trucks, H. B. Schlegel, G. E. Scuseria, M. A. Robb, J. R. Cheeseman, G. Scalmani, V. Barone, B. Mennucci, G. A. Petersson, H. Nakatsuji, M. Caricato, X. Li, H. P. Hratchian, A. F. Izmaylov, J. Bloino, G. Zheng, J. L. Sonnenberg, M. Hada, M. Ehara, K. Toyota, R. Fukuda, J. Hasegawa, M. Ishida, T. Nakajima, Y. Honda, O. Kitao, H. Nakai, T. Vreven, J. A. Montgomery, Jr., J. E. Peralta, F. Ogliaro, M. Bearpark, J. J. Heyd, E. Brothers, K. N. Kudin, V. N. Staroverov, R. Kobayashi, J. Normand, K. Raghavachari, A. Rendell, J. C. Burant, S. S. Iyengar, J. Tomasi, M. Cossi, N. Rega, J. M. Millam, M. Klene, J. E. Knox, J. B. Cross, V. Bakken, C. Adamo, J. Jaramillo, R. Gomperts, R. E. Stratmann, O. Yazyev, A. J. Austin, R. Cammi, C. Pomelli, J. W. Ochterski, R. L. Martin, K. Morokuma, V. G. Zakrzewski, G. A. Voth, P. Salvador, J. J. Dannenberg, S. Dapprich, A. D. Daniels, Ö. Farkas, J. B. Foresman, J. V. Ortiz, J. Cioslowski, and D. J. Fox, Gaussian, Inc., Wallingford CT, 2009.[2] Y. Zhao, D.G. Truhlar, *J. Chem. Phys.* 2006, **125**, 194101.

[3] M. M. Francl, W. J. Pietro, W. J.; Hehre, J. S. Binkley, M. S. Gordon, D. J. Defrees, J. A. Pople, *J. Chem. Phys.* 1982, **77**, 3654.

[4] a) E. Runge, E. K. U. Gross, *Phys.Rev.Lett.* 1984, **52**, 997, b) E. K. U. Gross, W. Kohn, *Adv. Quantum Chem.* 1990, **21**, 255. c) E. K. U. Gross, R. M. Driezler, (Eds.), Plenum Pres, New York, 1995; p.149.

[5] M. E. Casida, *Recent Advances in Density Functional Methods, Part I* (Ed.; D. P. Chong), World Scientific, Singapore, **1995**, p.115.

[6] J. B. Foresman, M. Head-Gordon, J. A. Pople, M. J. Frisch, *J. Phys. Chem.*, 1992, **96**, 135.

[7] S. Portmann, H. P. Lüthi, *Chimia* 2000, **54**, 766.